

Batch Crystallization of KCl: the Influence of the Cooling and Mixing Rate on the Granulometric Properties of Obtained Crystals

J. Prlić Kardum, A. Sander, and A. Glasnović

Faculty of Chemical Engineering and Technology, University of Zagreb, Marulicev trg 19, 10 000 Zagreb, Croatia; tel., fax: +385 1 4597 259, email: jprlic@fkit.hr, asander@fkit.hr, aglasnov@fkit.hr,

Original scientific paper

Received: July 7, 2004

Accepted: November 1, 2004

The influence of the intensity of mixing (100–500 rpm) and three different cooling rates on crystallization kinetics of KCl and granulometric properties of produced crystals has been investigated on a laboratory scale batch crystallizer. Different process conditions result with different crystal size distribution and crystal shapes. Obtained results show that cooling rate influences the supersaturation rate more intensively, the kinetics curves, and the average crystal size. On the other hand, crystal habit changes more with the intensity of agitation. Crystal size distribution can be expressed by log-normal distribution, i.e. its characteristic parameters, d_{50} and σ . Population density of crystal nuclei and overall linear growth rate are evaluated from crystal size distribution. The influence of cooling rate on both quantities (n^0 , \dot{L}) is more intense than the influence of mixing rate.

Keywords:

Crystallization, crystal habit, crystal size distribution, KCl, kinetics

Introduction

Crystallization is one of the basic processes in the final treatment of products in the chemical industry. Batch crystallization is an important unit operation in the chemical, photographic, and many other industries as manufacturing process to prepare a wide variety of crystalline products. Of the various types of batch crystallizer, cooling crystallization is one of the most common modes used in industry. Optimal operation is important in ensuring the efficiency of the overall process. Control of crystal quality (crystal size distribution, shape and crystal purity) is of special interest in crystallization processes and it is challenging due to the complexity and non-linearity of the process.

Many different variables (process conditions) influence the kinetics of crystallization and product properties, so that relations should be investigated experimentally. Consequently, experimental data doesn't always follow the theoretical principles.

The crystallization process consists essentially of two stages which generally proceed simultaneously but which can, to some extent, be independently controlled. The first stage is the formation of small particles or nuclei, and second stage is the growth of the nuclei.¹ The driving force for both, nucleation and crystal growth is supersaturation. Generally speaking, the nucleation rate and the crystal growth rate increases with increasing degree of supersaturation. Process parameters, such as cooling rate and intensity of agitation affect the

supersaturation (width of metastable zone) and therefore the nucleation and growth rate. The influence of agitation on nucleation process is very complex. Mechanical disturbances can enhance nucleation, but that is not always true.² If the nucleation rate can be controlled, the size of the crystals can be adjusted, and this is the most important feature of the crystallization process.

The dimension and the shape of particulate product are important for several reasons. The efficiency of any process for production of a particulate material relies on the size, shape, and size distribution.³ This is understandable, as the diameter of the crystals and their distribution is one of the criteria that determine the ease of further treatment (separation, drying and, frequently, also applications). It has been found that the crystal size distribution can be used for evaluation of a number of fundamental kinetic parameters useful, both, in the description of crystallization processes and in a design of crystallization equipment.⁴

The connection between the kinetics of nucleation and crystal size distribution is very complicated. Bransom et al. were the first to suggest that the kinetic data could be obtained from the distribution of crystal sizes, and they expressed the distribution of particle size in terms of quantity taken from mathematical statistics – the population density.⁵ Use of this quantity replaced distribution of the sizes of discrete species by coherent function. Presently this method is used regularly as a very

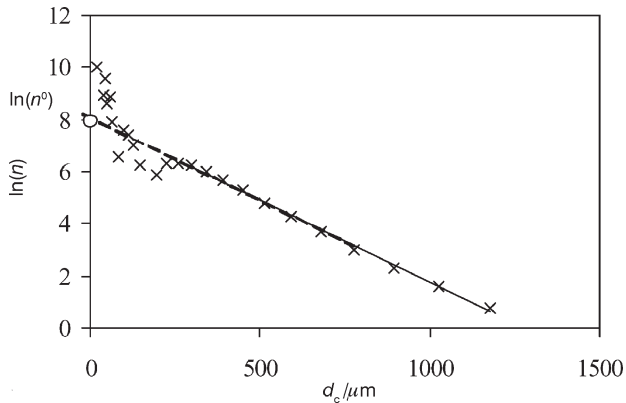


Fig. 1 – Graphical representation of the population balance

useful instrument in the characterization of the function of a crystallization apparatuses.⁶

Stone and Randolph recommended the procedure to determine population density of crystal nuclei, n^0 and linear crystal growth rate, \dot{L} .⁷

$$\ln(n) = \ln(n^0) - \frac{d_c}{\dot{L} - t_L} \quad (1)$$

The habit of a crystal may be defined as the type of external shape which results from the different rates of growth of various faces. Under certain conditions of crystallization one set of faces may be induced to grow faster than the others, or the growth of another set of faces may be retarded. Crystals of one given substance produced by different methods may be completely dissimilar in appearance, even though still belonging to the same crystal system. One method of crystallization may favor an acicular (needle) habit, while another may give a tabular habit (plates or flakes). A large number of factors can affect the habit of a crystal, e.g. the type of solvent, the pH of the solution, the presence of impurities, the degree of supersaturation, the rate of cooling, the temperature of crystallization, the degree of agitation, and so on.³

The objective of this paper was to investigate the effects of the intensity of mixing and the cooling mode on the granulometric properties of KCl (crystal size distribution and shape of the crystal) and kinetics of crystallization of potassium chloride from water solution.

Experiment

Three sets of experiments (different temperature profiles) have been performed in a

jacketed batch crystallizer shown on Figure 2. The apparatus consists of, crystallizer equipped with mechanical pitched 45° turbine stirrer and four wall baffles (width of about 1/12th of the vessel), thermostat and refractometer. The inner diameter of crystallizer (flat bottom) is 0.97 m. Total volume of solution was 0.73 dm³ (216 g KCl were added in 600 g water). Turbine stirrer used in this study draws the material to be mixed from above, and generates axial flow in the vessel.

The cooling rates were controlled by circulating water from the thermostat. Crystallization of KCl by cooling from water solution was investigated for five different stirrer speeds: 100 rpm, 250 rpm, 350 rpm, 400 rpm and 500 rpm. The initial mass ratio of aqueous KCl solution ($\zeta_{\text{KCl}/\text{H}_2\text{O}} = 36/100$) was the same for all experiments. A saturated solution of KCl was prepared by dissolving definite amount of KCl in the distilled water. Solution was then heated above the equilibrium temperature to ensure that all amount of KCl is dissolved. To avoid presence of any impurities clear solution was filtered before putting it into crystallizer. Temperature of solution was measured by means of digital thermometer. The solute concentration was determined by means of refractometer,² and proven by gravimetric method (error: 0.1 – 0.7 %). Refractometer is connected on the same thermostat as the crystallizer to ensure as precise as possible determination of refractive index, since it is dependent on both, temperature and concentration.

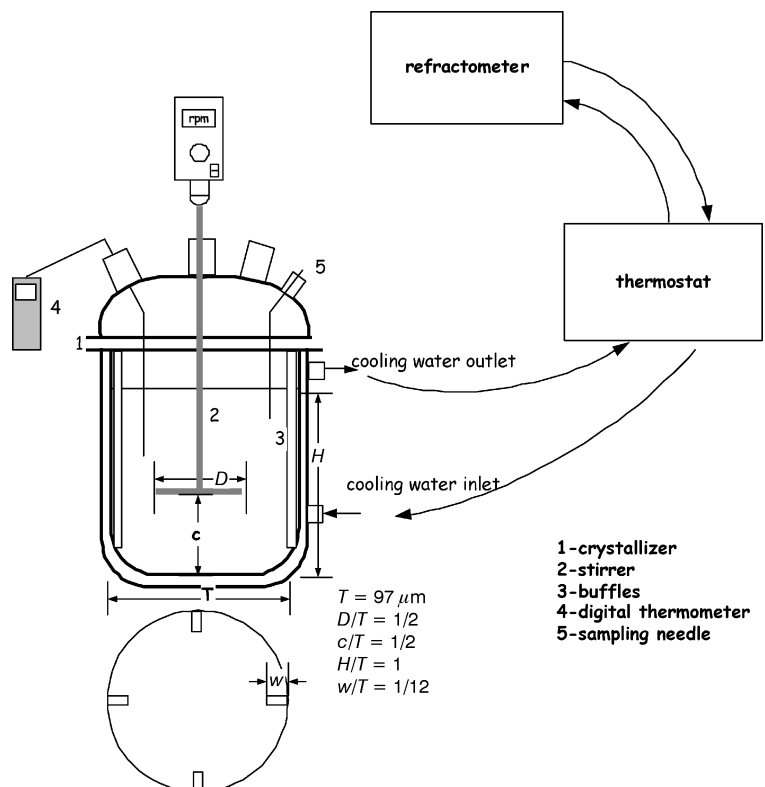


Fig. 2 – Experimental setup

Temperature profiles used in this investigation are shown of Figure 3. Two controlled linear temperature change (CR2, CR3) and one natural non-linear cooling rate (CR1) are chosen for investigation. For all cooling rates temperatures were lowered from 34 °C to 17 °C.

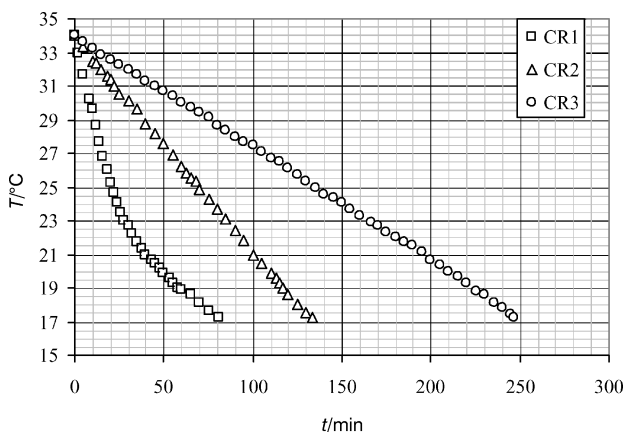


Fig. 3 – Cooling profiles used in this paper

Crystal size distribution was determined by laser diffraction method on Malvern Mastersizer 2000 (particle diameter range: 0.02 μm – 2000 μm). Except particle size distribution, information of specific surface area is obtained.

The shape of crystals was studied from photographs obtained on light microscope Olympus BX50.

It was determined the solubility curve of KCl in water, as a function of temperature for interval 34 °C – 17 °C.:

$$\zeta_{\text{KCl}/\text{H}_2\text{O}} = 27,86 + 0,28 \cdot T - 4,65 \cdot 10^{-7} \cdot T^2$$

Obtained results are in accordance with literature data.⁸

Results

The influence of the turbine stirrer speed and the cooling rate on a crystallization kinetics, crystal size distribution and obtained crystal habit, have been investigated on a laboratory scale.

Crystallization kinetics curves for a different stirrer speed are shown on Figure 4. Inside one set of experiments (one cooling rate) the shapes of the crystallization curves are pretty much the same. No general conclusion can be stated from those figures concerning the influence of agitation on the moment at which crystallization starts. The reason for that lies in the complexity of the way in what the agitation influences the nucleation process. Even thou mechanical disturbances enhance nucleation,

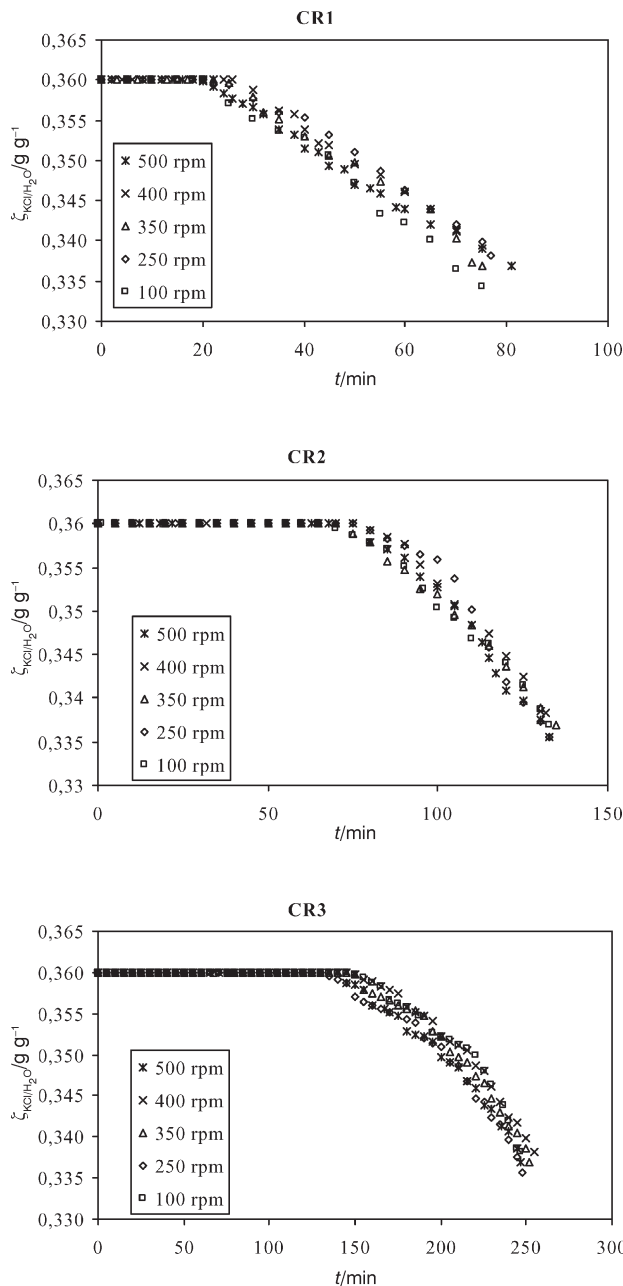


Fig. 4 – The influence of the turbine stirrer speed on the crystallization kinetics

Table 1 – Parameters of log-normal function and specific surface area

| Stirring speed | $d_{50} \cdot 10^{-4} \text{ m}$ | | | $s_m \cdot 10^{-2} \text{ m}^2 \text{ g}^{-1}$ | | | σ | | |
|----------------|----------------------------------|------|------|--|------|------|----------|------|------|
| | CR1 | CR2 | CR3 | CR1 | CR2 | CR3 | CR1 | CR2 | CR3 |
| 100 | 2.35 | 3.03 | 3.54 | 2.55 | 1.98 | 1.69 | 0.69 | 0.63 | 0.62 |
| 250 | 3.48 | 3.19 | 5.12 | 1.72 | 1.88 | 1.17 | 0.55 | 0.46 | 0.50 |
| 350 | 3.36 | 3.71 | 5.17 | 1.78 | 1.62 | 1.16 | 0.49 | 0.47 | 0.43 |
| 400 | 2.33 | 3.58 | 4.26 | 2.58 | 1.68 | 1.41 | 0.52 | 0.43 | 0.40 |
| 500 | 3.81 | 3.94 | 5.43 | 1.57 | 1.52 | 1.10 | 0.39 | 0.38 | 0.39 |

the increase in the intensity of agitation doesn't always lead to increase in nucleation.³ At low mixing rates, crystals are not agitated uniformly, so they are exposed to different hydrodynamics conditions. Only small crystals are mixed well. When crystals grow to specific size, it drops on the floor of the vessel and its growing rate is decreased. Well mixing of all present crystals (high mixing rates), insures favorable hydrodynamics conditions for mass transfer. This results in production of bigger crystals (Table 1) with more regular shape (Figure 11).

Supersaturation rate and maximal achieved supersaturation (Table 2) is not influenced in a great extend with mixing rates (Figure 5), so obtained crystal dimension is not affected in a great degree.

The cooling rate strongly influences the crystallization kinetics, as shown on Figure 6. At higher cooling rates crystallization starts earlier, for all investigated stirrer speeds. At the early stages of the crystallization process, the nucleation is dominating mechanism, since the crystallization is unseeded. For the fastest cooling rate (CR1) a maximum saturation is achieved for the shortest time. High supersaturation was generated at the beginning of the run, and low supersaturation near the end of the run.⁶ This results with high nucleation rate, formation of large numbers of nuclei and produced smaller crystals (Table 1). If supersaturation remains constant over a period of time (which were cases in cooling rate 2 and especially 3), nucleation is reduced and crystal growth is predominant (Figure 5).⁹ Once again, constant conditions for mass transfer are maintained at the same level (constant driving force), so crystals will grow. The peak in supersaturation can not be avoid in unseeded crystallization but choosing an appropriate cooling rate can modify the CSD of the final product.¹⁰ The average crystal dimension is increased with decreasing cooling rates for all mixing rates. (Table 1). Increase of the cooling rate shifts supersaturation curve towards lower temperatures, and the width of metastable zone is also increased. Consequently,

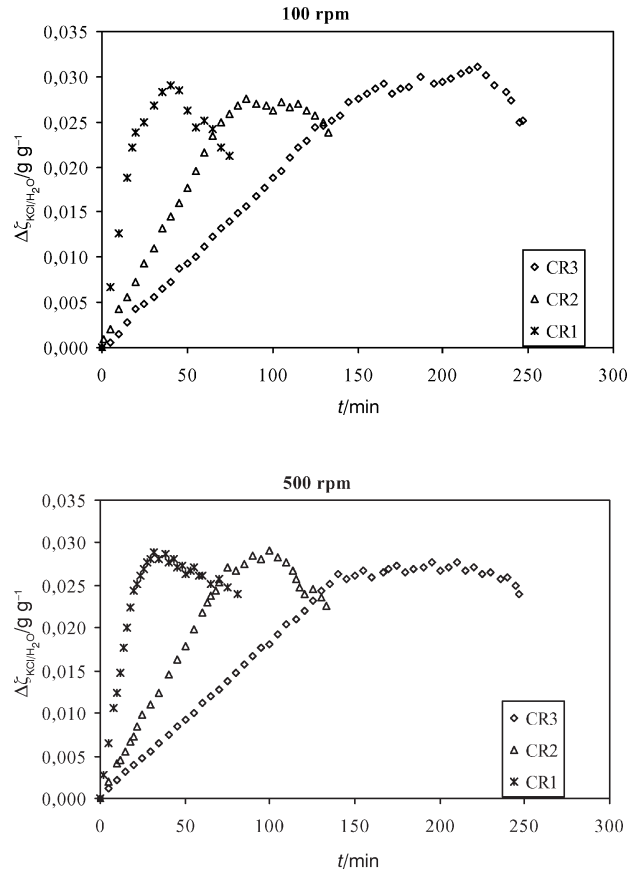


Fig. 5 – A course of the supersaturation for different cooling rates at low (100 rpm) and high (500 rpm) mixing rates

nucleation starts at lower temperature and less stable shapes and smaller crystals are produced.

Crystal size distribution is also affected by, both, intensity of agitation and cooling rates, figures 7 and 8. Crystal size distribution follows the log-normal function. Measure of particle diameter range, d_{50} , and measure of spread, σ , for all process conditions are shown in table 1. Narrower ranges of crystal sizes (smaller values of σ) are obtained for a higher stirrer speed and slower cooling rate. Symbols on Figures 7 and 8 represent the crystal size

Table 2 – The supersaturation rate and maximal supersaturation for all investigated process conditions

| Stirring speed | $d\zeta_{\text{KCl}/\text{H}_2\text{O}}/dt$ kg kg ⁻¹ min ⁻¹ | $\Delta\zeta_{\text{HCl}/\text{H}_2\text{O}}^{\text{max}}$ kg kg ⁻¹ | $d\zeta_{\text{KCl}/\text{H}_2\text{O}}/dt$ kg kg ⁻¹ min ⁻¹ | $\Delta\zeta_{\text{HCl}/\text{H}_2\text{O}}^{\text{max}}$ kg kg ⁻¹ | $d\zeta_{\text{KCl}/\text{H}_2\text{O}}/dt$ kg kg ⁻¹ min ⁻¹ | $\Delta\zeta_{\text{HCl}/\text{H}_2\text{O}}^{\text{max}}$ kg kg ⁻¹ |
|----------------|--|---|--|---|--|---|
| | cooling rate 1 | | cooling rate 2 | | cooling rate 3 | |
| 100 | $1.224 \cdot 10^{-3}$ | $2.888 \cdot 10^{-2}$ | $3.532 \cdot 10^{-4}$ | $2.911 \cdot 10^{-2}$ | $1.863 \cdot 10^{-4}$ | $2.765 \cdot 10^{-2}$ |
| 250 | $1.210 \cdot 10^{-3}$ | $3.154 \cdot 10^{-2}$ | $3.495 \cdot 10^{-4}$ | $2.967 \cdot 10^{-2}$ | $1.847 \cdot 10^{-4}$ | $3.077 \cdot 10^{-2}$ |
| 350 | $1.217 \cdot 10^{-3}$ | $2.955 \cdot 10^{-2}$ | $3.615 \cdot 10^{-4}$ | $2.726 \cdot 10^{-2}$ | $1.866 \cdot 10^{-4}$ | $2.994 \cdot 10^{-2}$ |
| 400 | $1.215 \cdot 10^{-3}$ | $3.192 \cdot 10^{-2}$ | $3.560 \cdot 10^{-4}$ | $3.141 \cdot 10^{-2}$ | $1.853 \cdot 10^{-4}$ | $3.110 \cdot 10^{-2}$ |
| 500 | $1.245 \cdot 10^{-3}$ | $2.911 \cdot 10^{-2}$ | $3.630 \cdot 10^{-4}$ | $2.761 \cdot 10^{-2}$ | $1.854 \cdot 10^{-4}$ | $2.821 \cdot 10^{-2}$ |

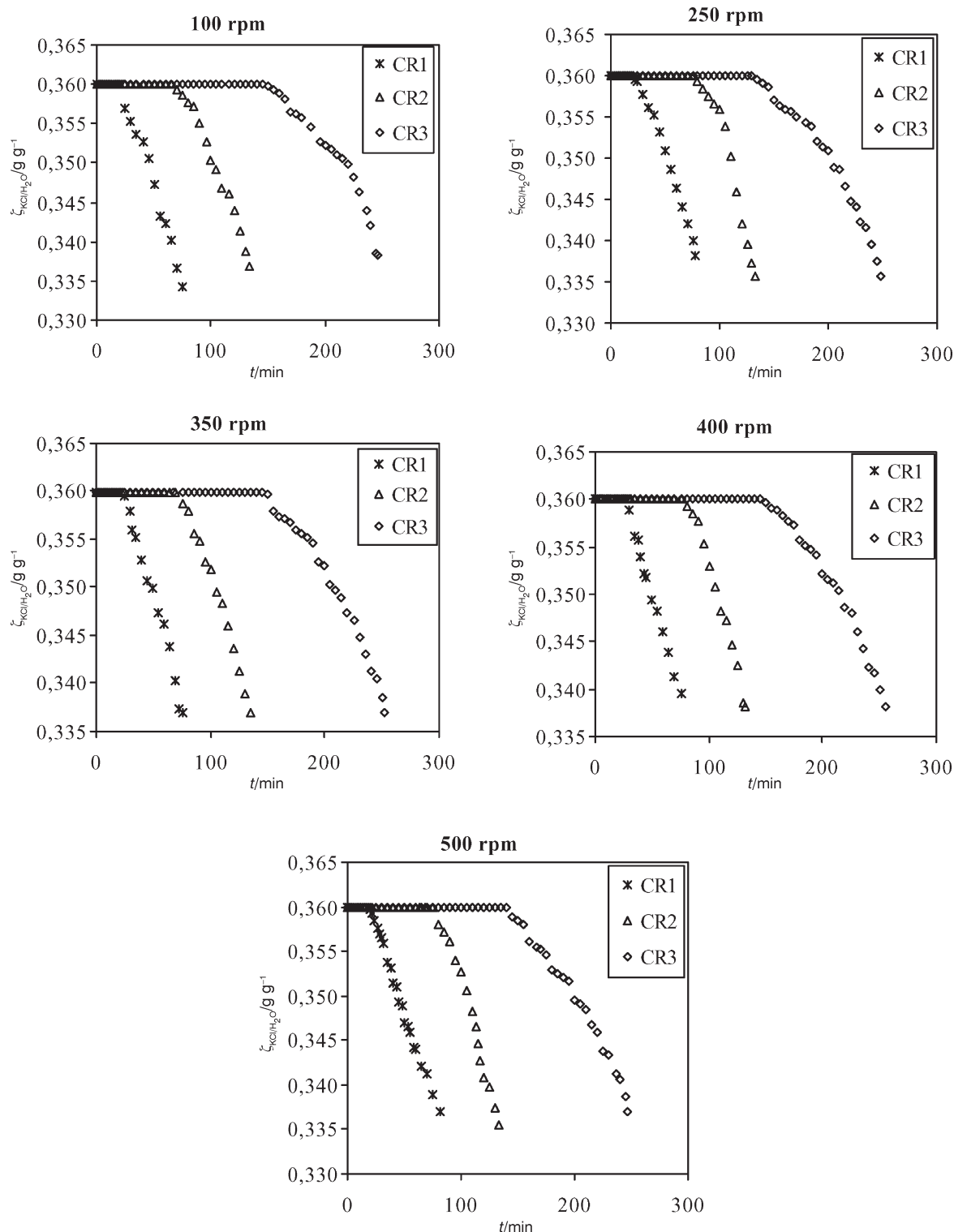


Fig. 6 – The influence of the cooling rates on the crystallization kinetics

distribution of industrially prepared KCl. Stirrer speed of 250 rpm and the medium cooling rate (CR2) probably corresponds to conditions at which KCl is produced originally.

Population density of crystal nuclei and overall linear growth rate are evaluated according to procedure suggested by Stone and Randolph⁴. Obtained

results are shown on Table 3. With regard to the influence of the cooling rate and mixing intensity on the supersaturation, conditions that expand the metastable zone (fastest cooling rate and lower agitation) result with higher supersaturation and higher linear growth rate. Although, slower cooling rate produces greater d_{50} , linear growth rate is higher at

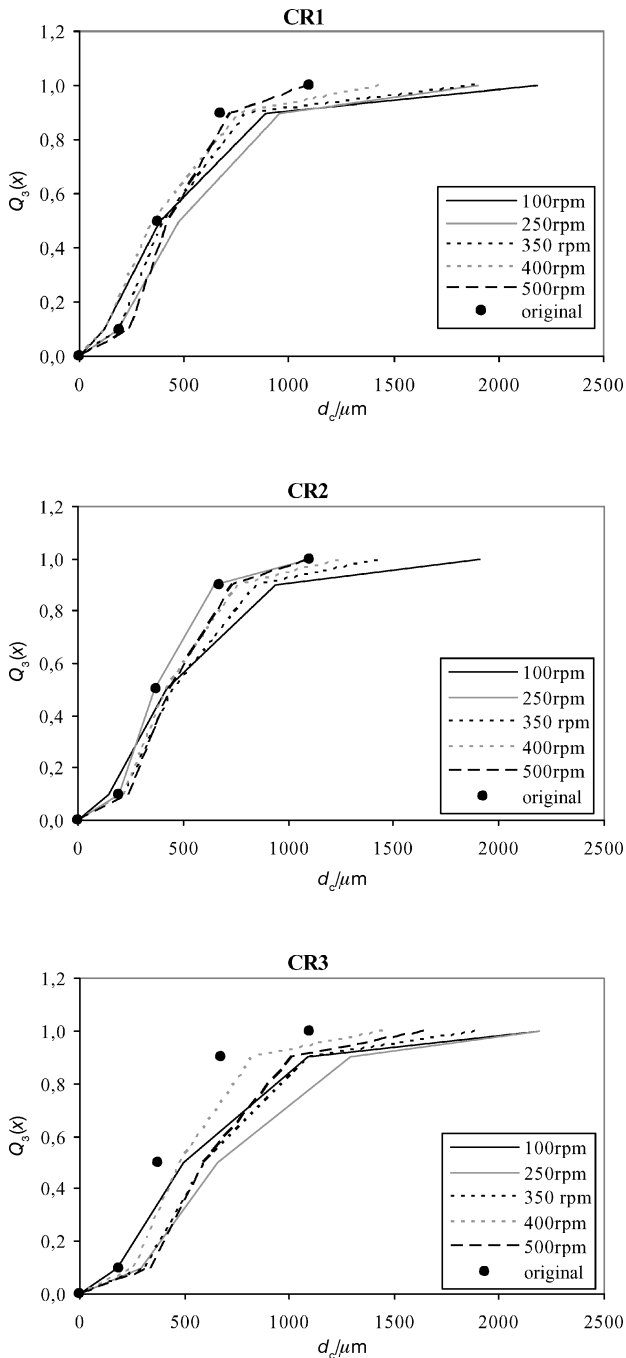


Fig. 7 – Crystal size distribution for different mixing rates

cooling rate 1. That can be explained with the shape of obtained crystals (crystal growth rate dominant in one direction). At cooling rate 1 (especially at 100 and 250 rpm) crystals are more irregular (acicular shape). The influence of cooling rate is more intense than the influence of mixing rate. Population density of crystal nuclei is increased for higher intensity of agitation.

Among many factors that can affect the habit of a crystal, the rate of cooling and the degree of agitation, will be discussed here. Different process conditions result with different crystal shapes (Figures 9 to 11).¹¹ Rapid cooling of a solution at 100 rpm (CR1) causes the preferential growth of a crystal in one particular direction, leading to the formation of needles. An acicular crystal habit (needle) is disliked in commercial crystals because of difficulties in the handling of the material. Needles tend to break down.³ For a given intensity of mixing (100 rpm, 500 rpm) slower controlled rate of cooling results in the production of crystals of regular shape (cubic). At 100 rpm, the shape of crystals changes from needles to rectangle, if cooling rate is lowered from CR1 to CR3. For a constant cooling rate (CR3) with increasing intensity of agitation crystal habit also changes from acicular to cubic. At 250 rpm different shapes of crystals are obtained (needle, rectangle, and cube). This may be the reason for aberration in the crystal size distribution and average sizes of produced crystals.

Conclusion

Change of cooling rate and intensity of mixing influences the kinetics of crystallization (population density of crystal nuclei and overall linear growth rate) and granulometric properties (crystal size distribution, crystal shape) of produced crystals.

Well mixing of all present crystals (high mixing rates) insures favorable hydrodynamics conditions for mass transfer. This results with production of bigger crystals with more regular shape (cube).

Table 3 – The population density of crystal nuclei, n^0 , and overall linear growth rate, L for all investigated process conditions

| Stirring speed n/min^{-1} | Cooling rate 1 | | Cooling rate 2 | | Cooling rate 3 | |
|---------------------------------------|----------------|---------------------------------|----------------|---------------------------------|----------------|---------------------------------|
| | n^0 | $\dot{L}, \mu\text{m min}^{-1}$ | n^0 | $\dot{L}, \mu\text{m min}^{-1}$ | n^0 | $\dot{L}, \mu\text{m min}^{-1}$ |
| 100 | 1139 | 2.610 | 1677 | 1.35 | 726 | 0.896 |
| 250 | 1144 | 2.582 | 6069 | 1.058 | 375 | 1.099 |
| 350 | 3527 | 2.053 | 1979 | 1.327 | 734 | 0.934 |
| 400 | 1966 | 2.224 | 2652 | 1.257 | 2710 | 0.658 |
| 500 | 3670 | 1.961 | 3496 | 1.228 | 956 | 0.898 |

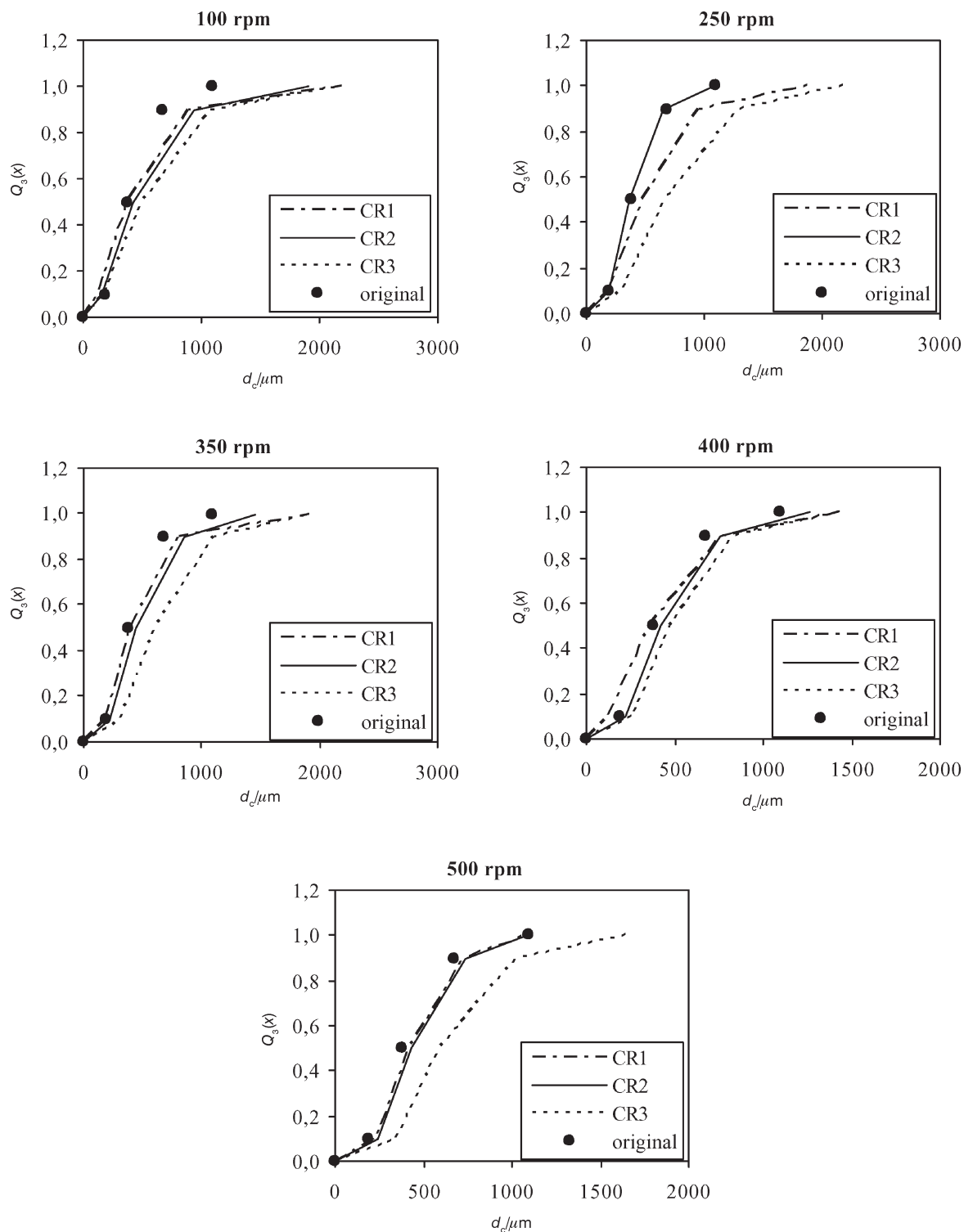


Fig. 8 – Crystal size distribution for different cooling rates

The cooling rate influences strongly the crystallization kinetics. At higher cooling rates crystallization starts earlier, for all investigated stirrer speeds. Increase of the cooling rate shifts supersaturation curve towards lower temperatures, and

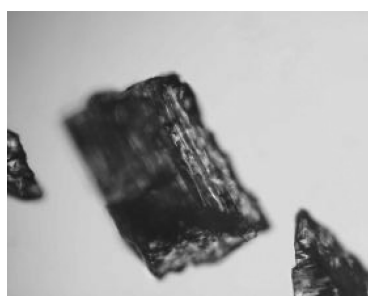
the width of metastable zone, is also increased. Consequently, nucleation starts at lower temperature and less stable shapes (needle) and smaller crystals are produced.



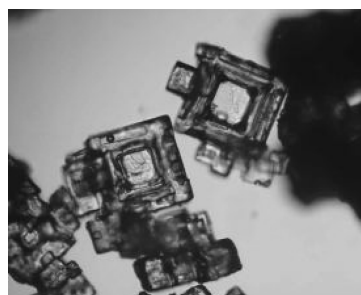
cooling rate 1



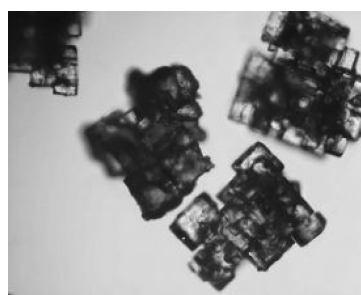
cooling rate 2



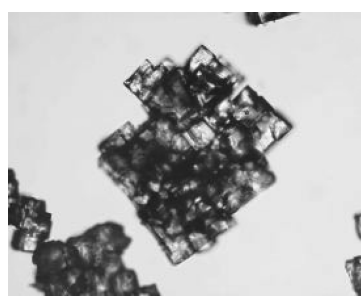
cooling rate 3



cooling rate 1



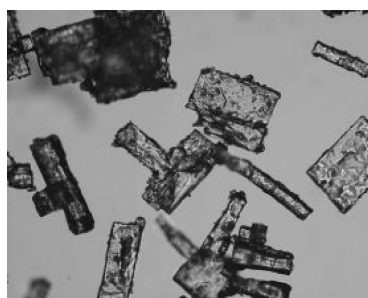
cooling rate 2



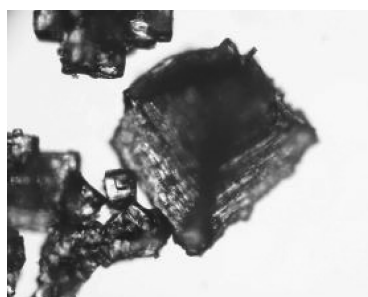
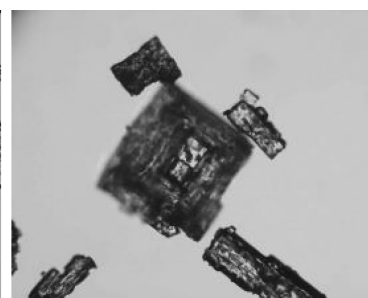
cooling rate 3

Fig. 9 – Shape of obtained crystals at different cooling rates (100 rpm)

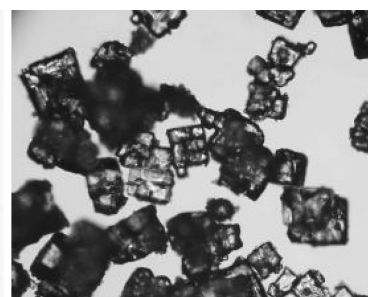
Fig. 10 – Shape of obtained crystals at different cooling rates (500 rpm)



250 rpm



350 rpm



400 rpm

Fig. 11 – Shape of obtained crystals at different mixing rate (CRI)

Notation

- \dot{L} – overall linear growth rate, m min⁻¹
 n – population density of crystals
 n^0 – population density of crystal nuclei
 $Q_3(x)$ – cumulative volume fraction of particles smaller than x
 s_m – specific surface area, m² g⁻¹
 t – time, min
 t_L – total crystallization time, min
 T – temperature, °C
 d_c – crystal diameter, m
 d_{50} – measure of particle diameter range (log-normal function), m
 $\zeta_{\text{KCl}/\text{H}_2\text{O}}$ – mass ratio, kg kg⁻¹
 $\Delta\zeta_{\text{KCl}/\text{H}_2\text{O}}$ – supersaturation mass ratio, kg kg⁻¹
 \dot{T} – cooling rate, EC min⁻¹

Greek symbols

- σ – measure of spread (log-normal function)

References

1. *Coulson, J. M., Richardson, J. F., Backhurst, J. R., Harker, J. H.*, Chemical Engineering, Pergamon Press, Oxford, 1978, pp. 689–710.
2. *Mullin, J. W., Raven, K. D.*, Influence of mechanical agitation on the nucleation of aqueous salt solutions, *Nature*, London, 1962.
3. *Mullin, J. W.*, Crystallisation, Butterworths & Co Ltd, London, 1970.
4. *Nyvtl, J., Sohnle, O., Matuchova, M., Broul, M.*, The Kinetics of Industrial Crystallization, Academia Prague, Prague, 1985.
5. *Bransom, S. H., Brown D. E., Heeley G. P.*, Crystallization Studies in Continuous Flow Stirred Tank Crystallizers, Industrial Crystallization, Symp., London, 1969.
6. *Myerson, A. S.*, Handbook of Industrial Crystallization, Butterworth-Heinemann, New York, 1993.
7. *Stone, P., Randolph, A. D.*, Chem. Eng. Progr. Symp. Ser. 65, 1969, No 95, 24.
8. *Rohani, S., Haeri, M., Wood, H. C.*, Comp. and Chem. Eng. **23** (1999) 263.
9. *Machej, K.*, Chem. Eng. and Proc. **36** (1997) 185.
10. *Mohameed, H. A., Abu-Jdayil, B., Al Khateeb, M.*, Chem. Eng. and Proc. **41** (2002) 297.
11. *Dirksen, J. A., Ring, T. A.*, Chem. Eng. Sci. **46** (1991) 2427.